Nanoscale

Accepted Manuscript

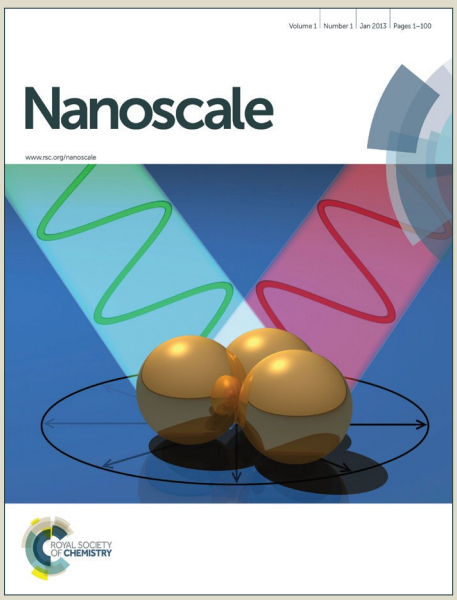

ROYAL SOCIETY OF CHEMISTRY

www.rsc.org/nanoscale

Journal Name

COMMUNICATION

Three-dimensionally grown thorn-like Cu nanowire arrays by fully electrochemical nanoengineering for highly enhanced hydrazine oxidation†

Received 00th January 20xx,
Accepted 00th January 20xx

DOI: 10.1039/x0xx00000x

www.rsc.org/

Jianfei Huang, Shunan Zhao, Wei Chen, Ying Zhou, Xiaoling Yang, Yihua Zhu* and Chunzhong Li*

This communication reports fully electrochemical nanoengineering toward three-dimensionally grown thorn-like Cu nanowire arrays (CNWAs) as a highly efficient and durable electrocatalyst for hydrazine oxidation. Characterized by substantial negative shifting of onset potential and enlarged catalytic current density, the CNWAs afforded greatly enhanced hydrazine oxidation activity, even transcending that of the Pt/C catalyst at higher reaction rate. Parameters of electrochemical engineering and metallization methods were found essentially influential on the microstructure, and thus the electrocatalytic activity of the CNWAs. The present work typifies a flexible and expandable route toward integrated electrodes of metallic 1D nanostructures which is of interest to advancing performances of cutting-edge electrochemical applications.

Persistent dedications were devoted in the past decades to alternative energy technologies in addressing possible depletion of fossil fuels and their environmental impact. In this endeavor, fuel cells stand out as an appealing power source.[1,2] Direct liquid fuel cell (DLFC) is one subcategory with commendable feasibility as fuels in liquid form are carried more readily.[3] Hydrazine-powered DLFC, featuring high theoretical voltage of 1.56 V, produces only water and nitrogen with no undesirable species that may poison electrocatalysts, and therefore has drawn wide research interests since its inception four decades ago.[4,5] A hinge to hydrazine-powered DLFC is active and durable hydrazine oxidation reaction (HzOR) electrocatalyst, research on which has involved catalytically active noble metals including Pt, Pd and Au.[6-8] Untowardly, scarcity of noble metals casts doubt on their massive implementation. Consequently, economical substitutes such as earth-abundant transition metals, doped carbon materials and metal/carbon hybrids have been proposed.[9-14] Owing to low cost and inherent active redox transformation, Cu-based catalysts have received attention as a potential candidate for catalyzing HzOR. For instance, Cu nanocubes/graphene composite was recently investigated as independent HzOR catalytic electrode, which demonstrated irreversible oxidation of hydrazine, as well as existence high-valence Cu as electron-shuttling mediator for HzOR.[12] Practical competence for DLFC has also been demonstrated in a Cu air/hydrazine full cell assembled with nanostructured Cu anodes, which was able to continuously operate up to 500 h.[1]

Aligned 1D nanostructures (e.g. nanowire arrays, NWAs) are enjoying growing preference as the electrode architecture in rechargeable batteries,[16] fuel cells,[17] chemical sensors[18] and electro-to-chemical cells,[19] because synergetic combination can be elegantly achieved for defined charge transport path along the 1D axial direction of nanowire and shortened mass diffusion length resulting from the opened space within the aligned arrays. Moreover, with direct preparation on current collectors, typical drawbacks in application of polymer binders for building nanostructured electrodes including blocking of active sites, hindered mass transport, aggregation and flaking-off of active materials are also favorably avoided.[20-22] Nevertheless, in contrast to previous success in synthesizing semiconductor (mainly metal oxides) NWAs on various sophisticated substrates by hydrothermal and vapor growth methods, preparation of metallic NWAs has been limited to electrodeposition using template membranes with channel-like pores.[16,23] Such protocols are poorly adaptable to non-planar conductive substrates in the form of foam, twisted wires and fabrics, which are playing increasingly important roles in constructing durable electrodes for energy storage and conversion.[24-26] Hence, synthesis of metallic NWAs by facile techniques need to be fuelled by new strategies.

In this communication we present large-area thorn-like Cu nanowire arrays (CNWAs) realized through a designed route by fully electrochemical nanoengineering of the starting substrates regardless of their complex geometry, with no extraneous template or shape directing agents required. Directly applied HzOR electrocatalyst, the CNWAs offered

Key Laboratory for Ultrafine Materials of Ministry of Education, School of Materials Science and Engineering, East China University of Science and Technology, Shanghai 200237, China
Email: yhzhu@ecust.edu.cn; czli@ecust.edu.cn
†Electronic Supplementary Information (ESI) available: Experimental details, additional figures and table. See DOI: 10.1039/x0xx00000x

boosted catalytic kinetics and demonstrated excellent long-run stability.

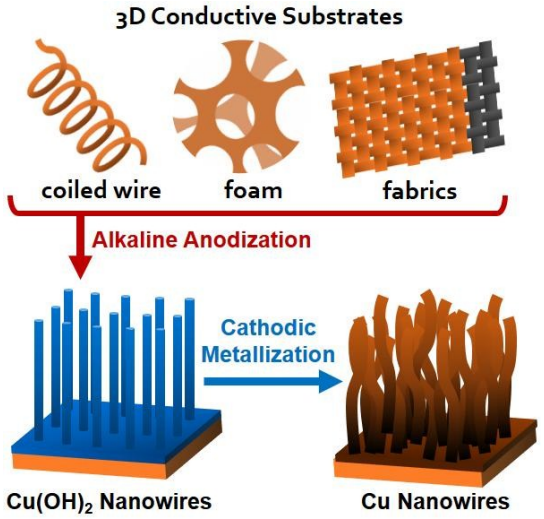

Fig. 1 Illustration of preparation of CNWAs on various 3D substrate *via* fully-electrochemical engineering.

The CNWAs were prepared *via* the scheme shown in Fig. 1 and the detailed steps are described in the Electronic Supplementary Information (ESI). Taking foamed Cu as an example, the starting substrate was first anodized in alkaline solution, and then cathodically metallized in neutral medium. Equipment set-ups and galvanostatic measurements are shown in Fig. S1. The anodization responsible for the formation of NWAs structure, where $Cu^{(II)}$ ions react with hydroxyl through olation reaction to grow $Cu(OH)_2$ crystal favorably along [100] direction,[27] requires appropriate concentration of OH^- and magnitude of current density for the targeted aligned 1D structure. Neutral medium or low current density was found favorable for side reactions leading to Cu_2O layer rather than $Cu(OH)_2$ NWAs (Fig. S2). The cathodization realized quasi-topological transformation of the nanostructure presumably back to metallic Cu, as may be speculated from the X-ray diffraction (XRD) patterns in Fig. 2. While three major characteristic peaks of cubic $Cu^{(0)}$ are seen for all samples, only the anodized Cu foam additionally gives diffraction peaks corresponding to $Cu(OH)_2$, suggesting successful reduction of $Cu(OH)_2$ to $Cu^{(0)}$. Surface state of the CNWAs was examined by X-ray photoelectron spectroscopy (XPS) shown in Fig. S3. The decoupled Cu 2p peaks at 932.3 and 952.0 eV can be indexed to $Cu^{(0)}$ or $Cu^{(I)}$, which are hard to differentiate because primary 2p peaks of Cu_2O and Cu are similar in position and shape.[28] However, peaks at higher energies of 934.8 and 954.2 eV associated with Cu 2p electrons of CuO species conclusively prove existence of surface oxidation. Two satellite peaks at 962.1 and 943.9 eV characteristic of Cu^{2+} are also vaguely identifiable, but their weak intensity compared to pure CuO suggests limited oxidation.[29] Such natural oxidation is in consistent with previous literatures, and the resulting high-valence Cu species may contribute to shuttling electrons for HzOR through the following reactions:[12,14,30]

$$N_2H_4 + 2OH^- \rightarrow [HO\text{-}H_2NNH_2\text{-}OH]^{2-} \quad (1)$$

$$[HO\text{-}H_2NNH_2\text{-}OH]^{2-} + 4CuO \rightarrow 2Cu_2O + 2H_2O + 2OH^- + N_2 \quad (2)$$

$$2Cu_2O + 4OH^- \rightarrow 4CuO + 2H_2O + 4e^- \quad (3)$$

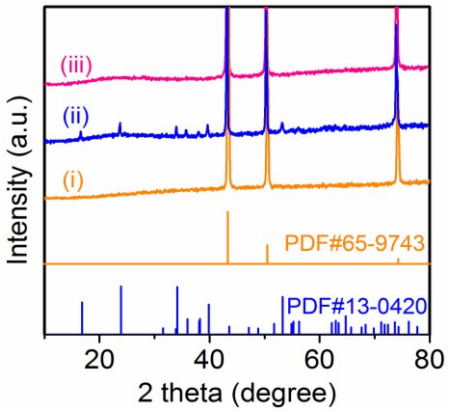

Fig. 2 XRD patterns of (i) Cu foam, (ii) anodized Cu foam and (c) CNWAs. The standard PDF patterns are of cubic structured Cu (#65-9743) and orthorhombic structured $Cu(OH)_2$ (#13-0420), respectively.

The morphology of the CNWAs was characterized by scanning electron microscopy (SEM) as shown in Fig. 3a,b. Dense coverage of the macroporous foam by CNWAs is obvious. Close-up view in Fig. 3b reveals that CNWAs possess curved outlines and throng analogous to thorns. To highlight the transformation of the NWAs structure from $Cu(OH)_2$ to Cu, in a typical procedure an anodized Cu foam was partially masked prior to cathodization, which thus remained partially unreduced due to lack of contact with electrolyte during the metallization process. Then we examined the area at the edge of the mask that was subsequently removed, as shown in Fig. 3c, in which the lower-right section stand the successfully transformed curved Cu nanowires while the protected $Cu(OH)_2$ nanowires are in the upper-left section. X-ray energy dispersive spectroscopy (EDS) elemental mapping of the region in the green square yielded Fig. 3d-f, which demonstrate the distinctively low oxygen content in the region of CNWAs. This result attests to the successful realization of the synthesis strategy. Further magnified view of the as-prepared Cu nanowires were presented in the transmission electron microscopy (TEM) image in Fig. S4a, and the diameter is around 100 nm. To further affirm the composition identity of the nanowires to be metallic Cu, we obtained selected area electron diffraction (SAED) pattern (inset of Fig. S4a), from which diffraction rings of (111), (222) and (220) planes of $Cu^{(0)}$ ascertain the metallic and polycrystalline nature of the nanowires. Diffraction ring corresponding to (111) plane of Cu_2O is also vaguely discernible. Consistently, a lattice spacing of 0.246 nm revealed in the high-resolution TEM image (Fig. S4b) was larger than that of (111) plane of Cu (0.208 nm) and can be assigned to (111) plane of Cu_2O, corroborating certain degree of surface oxidation of the Cu nanowires. The oxidation does not obscure the chemical identity of the metallic Cu nanowire as collaboratively confirmed by the XRD and SAED. In addition to its feasibility to CNWAs as demonstrated above, the present method is also of good flexibility in that not only Cu foam, for other spatially compl

conductive substrates such as strand of Cu coiled wires and carbon fabrics deposited with Cu layer, *in situ* grown Cu nanowires were also obtained (Fig. S5), with some modification to the method as detailed in the ESI.

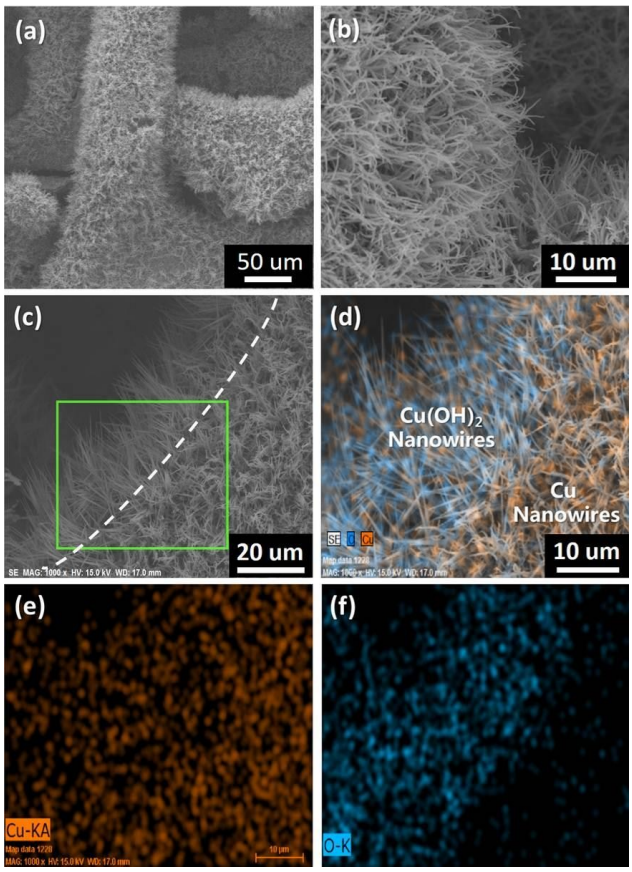

Fig. 3 SEM images of CNWAs at (a) low and (b) high magnifications. (c) SEM image of border area of $Cu(OH)_2$ and Cu NWAs, and the corresponding EDS elemental mapping of (d) Cu and O together, and of (e) Cu and (f) O, alone.

The electrochemical properties of CNWAs on the Cu foam were first probed by cyclic voltammetry (CV). As shown in Fig. 4a, while both CNWAs and Cu foam show two redox pairs characteristic of Cu(0)/Cu(I) and Cu(I)/Cu(II) conversions,[31] the CNWAs afforded considerably enlarged redox current density due to the massively increased electrode/electrolyte interface. CV profiles (Fig. S6) in the non-faradic potential window of the two electrodes show quasi-rectangular shape typically associated with electrical double layer capacitance (EDLC), which is proportional to the effective surface area (ESA) according to the following equation:[14]

$$C_{dl} = \varepsilon A/d$$

where C_{dl}, ε, A, and d stand for EDLC, permittivity, ESA and the effective thickness of the electrical double layer, respectively. Therefore, enhancement factor of ESA can be evaluated from the ratio of C_{dl} of the two electrodes, which was determined to be as high as 78. This greatly enlarged ESA is expected to bring considerable enhancement on electrochemical performance. To examine the HzOR electrocatalytic ability of the CNWAs, polarization data was collected, as shown in Fig. 4b with Cu foam and Pt/C catalyst as controls. Compared to the Cu foam, HzOR activity was greatly promoted: an HzOR onset was around –0.82 V (vs Ag/AgCl, the same for the following), ~140 mV negative to that of the Cu foam. Under an identical appli potential of –0.6 V, a limited current density of 7.8 mA/cm^2 was provided by Cu foam, while CNWAs afforded 150. mA/cm^2, corresponding to nearly 19-fold enhancement. The Pt/C control at approximately identical loading mass as the C nanowires offered the lowest onset potential, whose HzOR current density began to increase at –1.0 V, characterizing the excellent catalytic capability of Pt. In spite of this, its catalytic current increased much slower at elevated potentials and wa exceeded by the CNWAs at ~-0.665 V. This indicates that the CNWAs stand as a promising substitute for noble metal-free HzOR catalyst. Also, the CNWAs compare favorably with other previous reported HzOR catalysts (Tab. S1). We furthe investigated the influence of anodization and metallizatio processes on the microstructure and activity of the CNWA Short anodization durations led to insufficient growth of NWA structure (Fig. S7,S8), and thus predictably limi enhancement from the final product. Indeed, as summarized in Fig. 4c, the HzOR onset potentials and current densi derived from the polarization curves (Fig. S9) show that the HzOR performance is closely related to the anodizat durations. The optimized anodization duration is 30 min. I addition, it is also worth considering the effect of metallization process. Chemically reduced CNWAs (CR-CNWAs) wa obtained with $NaBH_4$ as reducing agent, which showed near identical HzOR onset potential as CNWAs (Fig. 4b). However upon increasing the potential, the CR-CNWAs generated lowe HzOR current. Consider the activity at –0.6 V, HzOR current of CR-CNWAs (119.7 mA/cm^2) is 79.5% of that of CNWAs (150. mA/cm^2). This is likely due to fast interaction of the precursor NWAs with the $NaBH_4$ under the wet-chemical condition causing fierce dissolution-crystallization and bubbling at the liquid/solid interface, leaving undesirable aggregates an disrupted morphology with the CR-CNWAs, as confirmed by SEM (Fig. S10). Occurrence of such aggregates leads to loss electrochemically active sites for HzOR, as evidenced by smaller ESA enhancement factor of CR-CNWAs (Fig. S6b). To further illustrate the kinetic boost, the Nyquist plots of CNWA and Cu foam are shown In Fig 4d. Both electrodes presente semicircles, suggesting similar electrocatalytic mechanism t followed a kinetically controlled behavior.[28] Diameter of th semicircle at high-frequency region is known as charge transfe resistance, R_{ct}, which is much smaller for the CNWAs indicating facilitated interfacial electron transfer for th CNWAs. For practical implementation in DLFC, resistance t destruction of catalyst materials is vital. Therefore, durabilit of the electrocatalyst was also examined. *J*-t curve (Fig. 4e) o the CNWAs over a period of 4000 s shows negligible 2.50 activity loss, half of which occurred during the initial 1/10 period (Fig. S11), demonstrating the long-run robustness of th CNWAs for HzOR. In contrast, the Pt/C electrode prepared by binder-involved drop casting not only affords lower activit but also sustains lower activity retention with loss of ~26.7%. Moreover, its *J*-t curve features a continuously decreasing profile which suggests unpromising stability. While b

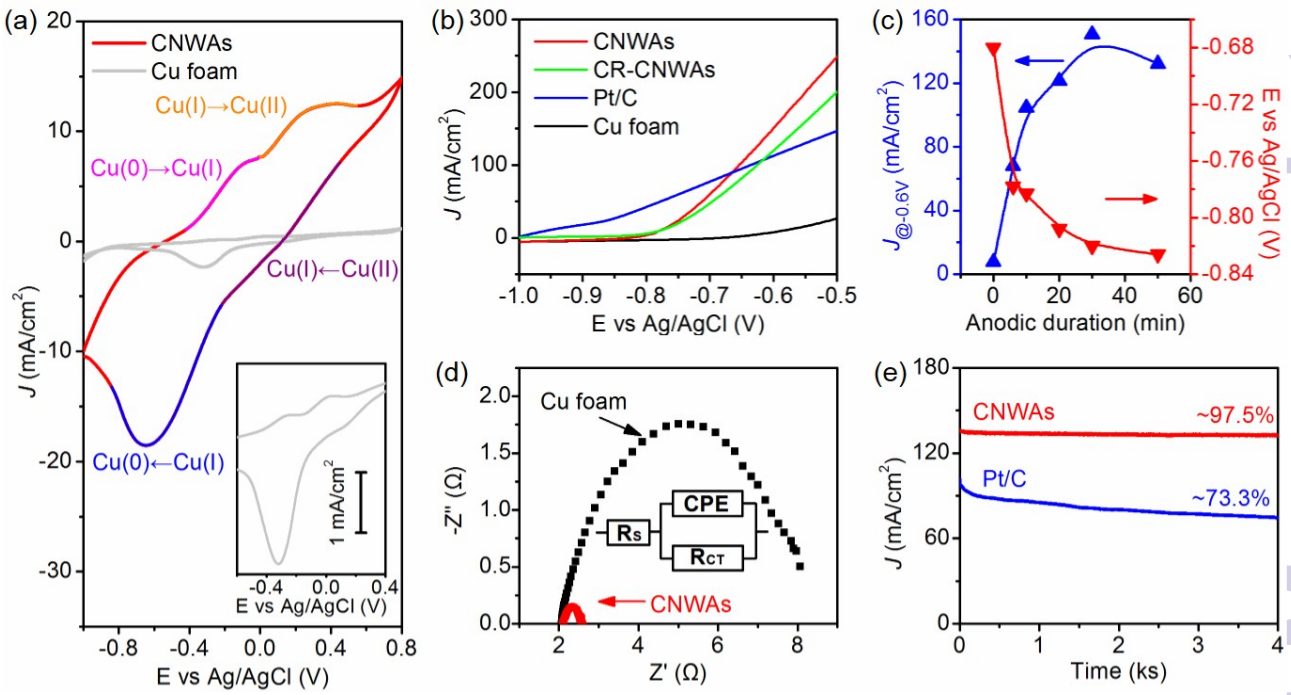

Fig. 4 (a) CV of CNWAs and Cu foam in 0.1 M phosphate buffer solution (PBS, pH 7.0). The inset is a magnified CV profile of Cu foam (b) Polarization curves of CNWAs, CR-CNWA Cu foam and Pt/C. (c) Current density at -0.6 V and HzOR onset potential of CNWAs prepared with various anodization duration. (d) Nyquist plots of CNWAs and Cu foam derived from AC impedance at an amplitude of 10 mV in a frequency range of 0.1-100k Hz at -0.6 V. The inset shows its equivalent circuit. (e) Chronoamperometric test for 4000 s at -0.6 for durability of CNWAs.

CNWAs and Pt/C electrodes employ nano/micro-sized catalysts, superior stability of the former may be benefited from the robust *in situ* growth and binderless electrode architecture, which effectively suppress flaking off or conglomeration of the effective composition/structure during the electrolysis where intense effervescence is involved. SEM characterization (Fig. 5) shows that the overall morphology of the CNWAs remained basically unchanged after the stability test, further confirming the CNWAs as a sturdy HzOR electrocatalyst.

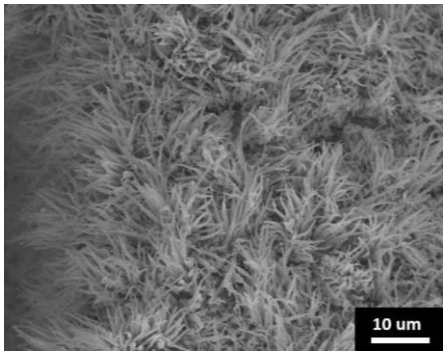

Fig. 5 SEM image of CNWAs after the HzOR chronoamperometric durability test.

In summary, three-dimensional thorn-like CNWAs were realized by a fully electrochemistry-processed method. The CNWAs were demonstrated to be a high-activity and sustainable HzOR electrocatalyst, offering greatly boosted electrode kinetics that featured early HzOR onset and high catalytic current density. Its competent electrocatalytic ability combined with the low cost of manufacturing, makes the platform promising for further hybridizing with other material to construct versatile free-standing nanostructured electrode serving various electrochemical applications.

Acknowledgements

This work was supported by the National Natural Scienc Foundation of China (21471056, 21236003, 21206042, an 21176083), the Basic Research Program of Shanghai (13NM1400700, 13NM1400701), and the Fundame Research Funds for the Central Universities.

Notes and references

1 B. C. H. Steele and A. Heinzel, *Nature*, 2001, **414**, 345.
2 M. K. Debe, Nature, 2012, 486, 43.
3 S. Park, J. M. Vohs and R. J. Gorte, *Nature*, 2000, **404**, 265.
4 G. E. Evans and K. V. Kordesch, *Science*, 1967, **158**, 1148.
5 H. Wang, Y. Ma, R. Wang, J. Key, V. Linkov and S. Ji, *Chem. Commun.*, 2015, **51**, 3570.
6 A. P. O'Mullane, S. E. Dale, J. V. Macpherson and P. R. Unwin *Chem. Commun.*, 2004, 1606.
7 Y. Liang, Y. Zhou, J. Ma, J. Zhao, Y. Chen, Y. Tang and T. Lu, *Appl. Catal., B*, 2011, **103**, 388.
8 X. Yan, F. Meng, Y. Xie, J. Liu, Y. Ding, *Sci. Rep.*, 2012, **2**, DOI:10.1038/srep00941.
9 J. Sanabria-chinchilla, K. Asazawa, T. Sakamoto, K. Yamada, Tanaka and P. Strasser, *J. Am. Chem. Soc.*, 2011, **133**, 5425.
10 T. Sakamoto, K. Asazawa, J. Sanabria-Chinchilla, U. Martinez, B. Halevi, P. Atanassov, P. Strasser and H. Tanaka, *J. Power Sources*, 2013, **247**, 605.

11 D. Yu, L. Wei, W. Jiang, H. Wang, B. Sun, Q. Zhang, K. Goh, R. Si and Y. Chen, *Nanoscale*, 2013, 5, 3457.
12 H. Gao, Y. Wang, F. Xiao, C. B. Ching and H. Duan, *J. Phys. Chem. C*, 2012, **116**, 7719.
13 Y. Meng, X. Zou, X. Huang, A. Goswami, Z. Liu and T. Asefa, *Adv. Mater.*, 2014, **26**, 6510.
14 C. Liu, H. Zhang, Y. Tang, S. Luo, *J. Mater. Chem. A*, 2014, **2**, 4580.
15 E. Granot, B. Filanovsky, I. Presman, I. Kuras and F. Patolsky, *J. Power Sources*, 2012, **204**, 116.
16 P. L. Taberna, S. Mitra, P. Poizot and P. Simon, *Nat. Mater.*, 2006, **5**, 567.
17 Z. Xia, S. Wang, Y. Li, L. Jiang, H. Sun, S. Zhu, D. S. Su and G. Sun, *J. Mater. Chem. A*, 2013, **1**, 491.
18 Q. Yan, Z. Wang, J. Zhang, H. Peng, X. Chen, H. Hou and C. Liu, *Electrochim. Acta*, 2012, **61**, 148.
19 K. Xu, F. Wang, Z. Wang, X. Zhan, Q. Wang, Z. Cheng, M. Safdar and J. He, *ACS Nano*, 2014, **8**, 846.
20 G. Wang, X. Lu, T. Zhai, Y. Ling, H. Wang, Y. Tong and Y. Li, *Nanoscale*, 2012, **4**, 3123–3127.
21 Y. Luo, J. Luo, W. Zhou, X. Qi, H. Zhang, D. Y. W. Yu, C. M. Li, H. J. Fan and T. Yu, *J. Mater. Chem. A*, 2013, **1**, 273.
22 D. Kong, J. Luo, Y. Wang, W. Ren, T. Yu, Y. Luo, Y. Yang and C. Cheng, *Adv. Funct. Mater.*, 2014, **24**, 3815.
23 M. T. Molares, V. Buschmann, D. Dobrev, R. Neumann, R. Scholz, I. U. Schuchert and J. Vetter, *Adv. Mater.*, 2001, **13**, 62.
24 W. Zhou, X.-J. Wu, X. Cao, X. Huang, C. Tan, J. Tian, H. Liu, J. Wang and H. Zhang, *Energy Environ. Sci.*, 2013, **6**, 2921;
25 P. Yang, Y. Ding, Z. Lin, Z. Chen, Y. Li, P. Qiang, M. Ebrahimi, W. Mai, C. P. Wong and Z. L. Wang, *Nano Lett.*, 2014, **14**, 731;
26 A.-L. Wang, X.-J. He, X.-F. Lu, H. Xu, Y.-X. Tong and G.-R. Li, *Angew. Chem., Int. Ed.*, 2015, **54**, 3669.
27 X. Wu, H. Bai, J. Zhang, F. Chen and G. Shi, *J. Phys. Chem. B*, 2005,**109**, 22836.
28 Z. Lu, M. Sun, T. Xu, Y. Li, W. Xu, Z. Chang, Y. Ding, X. Sun and L. Jiang, *Adv. Mater.*, 2015, **27**, 2361.
29 D. Tahir amd S. Tougaard, *J. Phys.: Condens. Matter*, 2012, **24**, 175002.
30 Z. Yin, L. Liu and Z. Yang, *J. Solid State Electrochem.*, 2011, **15**, 821.
31 M. Liu, R. Liu and W. Chen, *Biosens. Bioelectron.*, 2013, **45**, 206.